



Increased photovoltaic utilisation from direct current distribution: Quantification of geographical location impact

Downloaded from: <https://research.chalmers.se>, 2023-05-04 19:38 UTC

Citation for the original published paper (version of record):

Ollas, P., Thiringer, T., Chen, H. et al (2021). Increased photovoltaic utilisation from direct current distribution: Quantification of geographical location impact. *Progress in Photovoltaics: Research and Applications*, 29(7): 846-856. <http://dx.doi.org/10.1002/pip.3407>

N.B. When citing this work, cite the original published paper.

Increased photovoltaic utilisation from direct current distribution: Quantification of geographical location impact

Patrik Ollas^{1,2}  | Torbjörn Thiringer²  | Huijuan Chen¹  | Caroline Markusson¹ 

¹Department of Energy and Resources, RISE Research Institutes of Sweden, Borås, Sweden

²Department of Electrical Engineering, Chalmers University of Technology, Gothenburg, Sweden

Correspondence

Patrik Ollas, Department of Energy and Resources, RISE Research Institutes of Sweden, Borås, Sweden.
Email: patrik.ollas@ri.se

Funding information

Energimyndigheten, Grant/Award Number: 43276-1 and 47273-1

Abstract

In this paper, the performance of a direct current (DC) distribution system is modelled for a single-family residential building and compared with a conventional alternating current (AC) system to quantify the potential energy savings and gains in photovoltaic (PV) utilisation. The modelling is made for two different climates to quantify the impact of the geographical location. Results show that the system losses are reduced by 19–46% and the PV utilisation increased by 3.9–7.4% when using a DC distribution system compared to an AC equivalent, resulting in system efficiency gains in the range of 1.3–8.8%. Furthermore, it is shown that the geographical location has some effect on the system's performance and PV utilisation, but most importantly, the grid interaction is paramount for the performance of the DC topology.

KEYWORDS

battery storage, direct current (DC), energy savings, photovoltaic, PV load correlation, residential building

1 | INTRODUCTION

Power from photovoltaic (PV) panels is generated as direct current (DC) and batteries operate with DC, and almost all electronic loads in buildings are natively DC operated. In today's conventional alternating current (AC) systems with PV and battery storage, there are conversions between AC and DC required before the final user stage, and all these conversions are associated with electrical losses. By adopting a DC distribution network in the building, many of these conversion losses can be avoided and thus increase the system's performance and utilisation of the PV energy. Lately, there have been numerous attempts to determine whether DC is superior to AC in terms of energy efficiency on a system level and what circumstances affect these results. In Dastgeer et al.'s literature comparison of past and

present work in the area, one conclusion is that gains from in-house DC distribution differ greatly, varying from 1.3% to 20%, including studies that show no efficiency gain with DC supply.¹ However, as suggested by the same authors, comprehensive research efforts based on detailed modelling are needed further, given the importance of accurate assumptions of power electronic components and demonstrations to provide a true comparison between the two scenarios.

In previous work done by Ollas, comparing AC and DC topologies for a single-family house in Sweden equipped with solar PV and battery storage, it is concluded that the energy savings and utilisation of the generated PV energy increase for a topology with DC distributions.² Energy savings for the studied case were between 2.5% and 5.6%, and the PV utilisation increased by up to 10 percentage points. It was also concluded from the same study that the major loss

Abbreviations: AC, alternating current; cond, conduction; DC, direct current; DHW, domestic hot water; HVAC, heating, ventilation and air conditioning; KPI, key performance index; PCC, Pearson correlation coefficient; PFC, power factor correction; PV, photovoltaic.

This is an open access article under the terms of the Creative Commons Attribution License, which permits use, distribution and reproduction in any medium, provided the original work is properly cited.

© 2021 The Authors. Progress in Photovoltaics: Research and Applications published by John Wiley & Sons Ltd.

contribution for the DC topology came from the grid-tied inverter and that these losses could be minimised for cases where PV generation better coincides with the load demand. Other studies have also concluded that there is an energy-saving potential when switching to DC distribution in buildings³⁻¹⁰ and that the inclusion of PV and battery storage, as DC sources, are a prerequisite for obtaining these savings. Fregosi et al. performed a comparative modelling study of an AC and DC topology in commercial buildings across the USA and found that the largest gains were obtained in the more hot-humid climates.¹¹ Missing in this study is however the inclusion of battery storage that could further boost the system's self-consumption of PV energy and thus increase the energy savings for a DC topology. In a related study done on energy savings from direct-DC usage in US residential buildings, Vossos et al. have modelled the effect in 14 different cities, geographically spread throughout the USA.¹² This work acknowledges the load-dependent efficiencies, but it is not clear whether the whole working interval for the efficiency is considered at part-load conditions. A deficit from this study is also the usage of a constant roundtrip efficiency for the battery, which, together with the consideration of the part-load efficiencies of all converters, are acknowledged as areas for improvements.^{1,2} This paper reports on a continuation of Ollas' previous work,² in which the system is modelled in another climate, having a better correlation between supply (PV) and demand (load usage), to see how this affects the system's performance. It uses the measured household appliance data from a single-family house located in Sweden and modifies the heating, ventilation and air conditioning (HVAC) to a warmer climate using IDA Indoor Climate and Energy (IDA ICE) and modelled PV-generation profiles. The study also uses detailed characteristics in the modelling of the power electronic components and the battery obtained from laboratory measurements. This paper contributes to previous studies with a detailed modelling comparison of DC distribution networks in two different climates with their differences in HVAC demand profiles and PV generation and quantifies their respective energy savings and PV utilisation gains, concluding how much the geographical location impacts the system's performance. A sensitivity analysis is also made by altering the PV array and battery sizes to quantify its respective impact on the system's performance. Furthermore, this work also presents a quantification of the contributions from the different loss sources, to give an understanding of where to put the focus for future studies.

2 | THEORY

2.1 | AC and DC building topologies with a PV and battery system

Apart from in rural areas without a shared electrical grid, AC supply of buildings is today dominating the electric power supply to all types of buildings. Figure 1 shows a typical AC topology for a residential building, in this case also equipped with solar PV and battery storage. Today's household appliances are almost exclusively operated on DC at their final stage. Note that all converters are subject to losses where the AC/DC conversion is done in two steps: firstly rectification (AC/DC) and then DC/DC conversion to the desired DC voltage level,^{13,14} typically using a power factor correction (PFC) converter.

A worst-case scenario in Figure 1 involving a maximum number of conversion steps is when excess PV is inverted (DC/AC) and stored in the battery through two conversions: AC/DC and DC/AC, and then supplied to the big loads with additional DC/AC and AC/DC conversions, resulting in a total of four conversion steps. This can be illustrated using the power flow as^{*}

$$P_{load} = P_{pv} \cdot \eta_{DC/AC} \cdot \eta_{AC/DC} \cdot \eta_{DC/AC} \cdot \eta_{AC/DC} \quad (1)$$

PV is generated as DC, and the battery storage is operated using DC, and they are both AC coupled in this topology, that is, connected to the main AC link. An alternative approach is that the DC sources, that is, battery and PV array, are connected to a DC link as presented in Li and Danzer.¹⁵ Still, converters are needed, but the losses of a DC/DC converter are lower compared to the ones of an AC/DC converter.

In a DC topology (see Figure 2), the PV and battery stored energy are better utilised since they are both connected directly on the main DC link (i.e., DC coupled), and thus, the DC/AC stage is removed and replaced with a more efficient DC/DC converter.[†]

In comparison with the worst-case scenario from Figure 1, where PV energy is supplied to the loads through the battery storage, the equivalent conversion steps are reduced to three. For small power loads, an additional DC/DC conversion is needed for both topologies (see dashed perimeter in Figures 1 and 2) and is assumed equal in performance for both cases. Similar to (1), the efficiency for the power flow can be expressed as[‡]

$$P_{load} = P_{pv} \cdot \eta_{DC/DC} \cdot \eta_{DC/DC} \cdot \eta_{DC/DC} \quad (2)$$

2.2 | Electrical losses in residential buildings

There are two main electrical losses occurring in a residential building: conduction and conversion. Here, the underlying theory of these two sources is explained.

2.2.1 | Cable conduction losses

Cable conduction losses occur when power is transferred in the cables and is given, for each modelled time step t_k , as

$$p_{cond}(t_k) = 2ri(t_k)^2 \quad (3)$$

where the factor '2' is due to the return conductor and with i as the current throughput. The cable resistance, r , is determined by the cross-sectional area, A , resistivity (ρ) and cable length, l , as

$$r = \rho \frac{l}{A} \quad (4)$$

2.2.2 | Conversion losses

The conversion losses come from voltage conversions, rectification (AC/DC) and inversion (DC/AC). As few loads operate directly from the

^{*}Please refer to an online or colour-printed version for better visualisation of the stepwise conversions.

[†]In this study, a buck converter is used for DC/DC conversion with an efficiency of 98.5% and is placed between the main DC link voltage, the battery, and the PV array in the DC topology. Whereas in the AC topology, this conversion is done with an H-bridge, having an efficiency of 97%.

[‡]Please refer to an online or colour-printed version for better visualisation of the stepwise conversions.

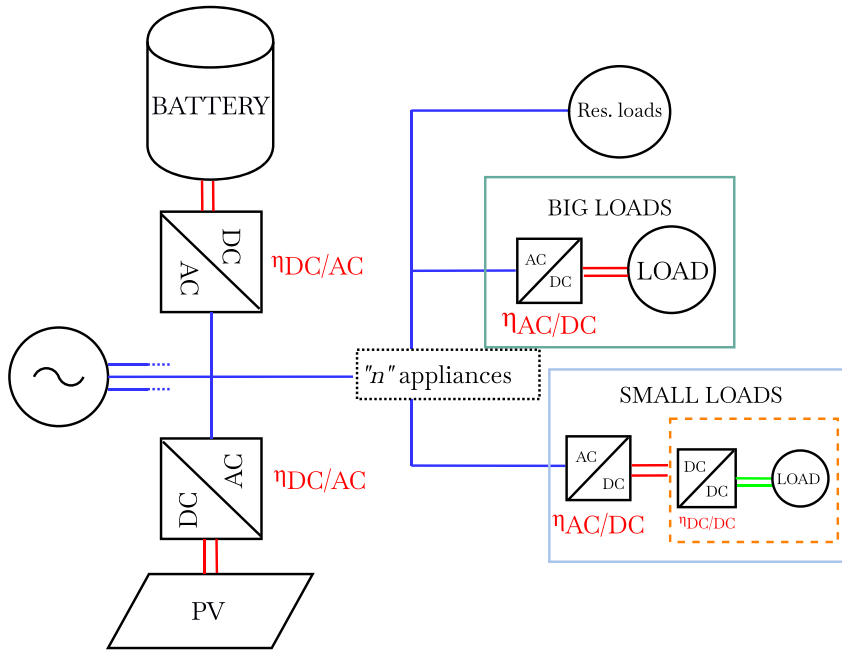


FIGURE 1 Typical AC topology with a PV and battery system. Dashed perimeter is the DC/DC conversion for the low-power appliances using a PFC and are equal for both the AC and DC scenarios. 'Res. loads' are resistive loads that can be operated on either AC or DC

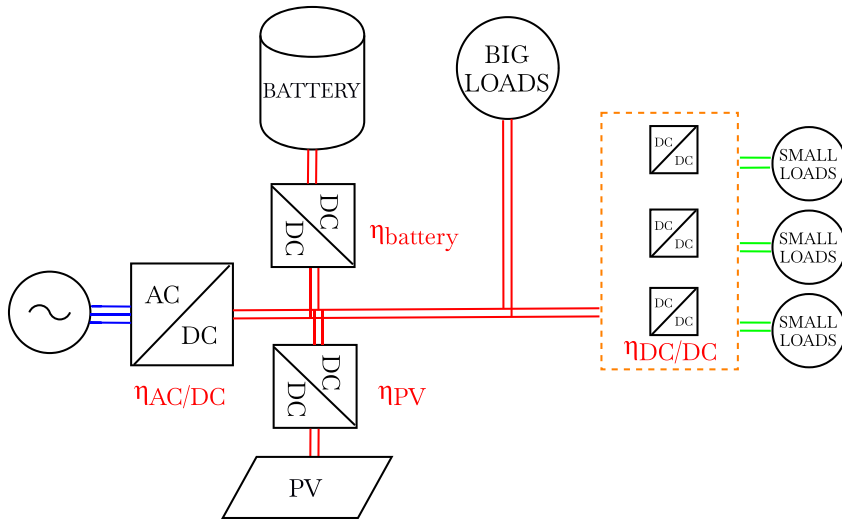


FIGURE 2 Example of a DC system topology with two DC voltage levels, including a PV array, battery storage and a bidirectional grid-tied converter, with the following colour coding for distribution: AC, 380 VDC and 24/48 VDC

supplied voltages (230/110 VAC or 380 VDC), conversions are needed, and the losses of these stem from the electronic components inside the respective converters. The losses are given by the converter's efficiency, η_{conv} , and are dependent on the converter's loading.

To determine the losses from a voltage conversion, the input and output quantities can be measured, and the difference is the losses. Single-phase AC and DC powers are given as

$$p_{AC}(t_k) = u_{AC}(t_k) i_{AC}(t_k) \quad (5)$$

$$p_{DC}(t_k) = u_{DC}(t_k) i_{DC}(t_k) \quad (6)$$

where $u_{AC}(t_k)$ and $i_{AC}(t_k)$ are the AC voltage and current, and $u_{DC}(t_k)$ and $i_{DC}(t_k)$ are the DC equivalents.

The conversion efficiency, assuming AC/DC conversion is given, using (5) and (6), as

$$\eta_{conv, AC/DC}(t_k) = \frac{p_{DC}(t_k)}{p_{AC}(t_k)} \quad (7)$$

The corresponding conversion losses are then given as

$$p_{conv}(t_k) = (1 - \eta_{conv, AC/DC}(t_k)) p_{load}(t_k) \quad (8)$$

where $p_{load}(t_k)$ is the converter power throughput for each time instance, t_k .

2.3 | Load and PV correlation

In Swedish residential buildings, the peak electricity usage normally occurs during the cold and darker months, caused mainly by a higher heating demand, which is addressed to a great extent using heat pumps. Also, the need for lighting is greater during the darker months. The main part of the electricity demand in Swedish residential buildings consists of electricity for heating and lighting, which leads to a modest demand during the warmer and lighter months and thus creates a poor correlation with the availability of PV energy. On the other side of the spectrum, other geographical locations have their peak electricity usage during the hotter and lighter periods of the year, caused by the need for cooling. This gives a better seasonal correlation with

the PV-generated energy than in countries like Sweden. Seasonal variations in supply (PV) and demand (load usage) are one thing, but it is also important to address the intraday correlation between these two when evaluating the performance of a PV system.

To quantify the natural match between PV generation and load demand, different correlation models can be used, and some of them are summarised in Ramadhani et al.¹⁶ In this study, the Pearson correlation coefficient (PCC) is used to calculate the correlation between the two continuous data sets of load usage and PV generation:

$$\rho(PV, Load) = \frac{1}{N-1} \sum_{i=1}^N \left(\frac{PV_i - \mu_{PV}}{\sigma_{PV}} \right) \left(\frac{Load_i - \mu_{Load}}{\sigma_{Load}} \right) \quad (9)$$

where μ_{PV} and σ_{PV} are the mean and standard deviations of the PV generation, respectively, and μ_{Load} and σ_{Load} are the ditto for the load usage, using N number of observations. The resulting correlation coefficient (-1 to $+1$) describes the linear relation between the two variables, where -1 represents a negative relation, for example, increasing and decreasing variables, respectively, and $+1$ a positive relation, for example, increasing and increasing.

3 | METHODOLOGY

In this section, the two used cases are presented together with the system modelling methodology, including key performance indexes (KPIs) and the investigated system topologies.

3.1 | Load and PV-generation profiles

In this study, data of load demand and PV generation are used from two different geographical locations: Borås, Sweden, and Phoenix, USA, which have two different load and generation (PV) characteristics. The first location has a poor correlation between PV generation and load demand, while the second location has a better correlation. Both studies are for a single-family residential building, and their characteristics are presented below. The modelled load demands are obtained from simulations using the IDA Indoor Climate and Energy (IDA ICE) software, with the building model adopted from Chen and Markusson¹⁷ and modified to represent a conventional Swedish single-family house with an average U -value of $0.26 \text{ W}/(\text{m}^2\text{K})$. For both cases, the energy demand from household appliances, for example, TV, cooking, cleaning and domestic hot water (DHW) usage, are assumed equal. The load for household appliances and DHW production were specified to be 30 and 25 kWh/m²/year, respectively, suggested by Levin et al.¹⁸ as standard values in Sweden for residential building energy simulations. Thus, the difference in electricity usage, in both space and time, comes from the HVAC equipment usage.

The HVAC usage simulated in IDA ICE is dependent on the type of system used, its operation and control. In the Swedish case, a ground-source heat pump (GSHP) with an electrical backup heater is used to provide both space heating and DHW. The GSHP has a rated capacity of 8.36 kW, and the modelling is done to keep the indoor temperature at a minimum of 21°C during the heating season. A balanced ventilation system with a rotatory heat exchanger is used, which is typical for single-family houses in Sweden. A constant supply flow rate of 60 L/s, corresponding to 0.386 L/s/m^2 is used. In the US case, the DHW is generated from a water heater using a resistive element,

TABLE 1 Energy demand and PV generation (both in AC quantities) and the Pearson correlation coefficient for difference loads at the two locations

	Borås, Sweden	Phoenix, USA
Energy demand (kWh)	10,744	11,946
PV AC energy (kWh)	3583	7077
PCC—all loads (—)	−0.31	−0.18
PCC—household appliances (—)	−0.23	−0.35
PCC—cooling (—)	—	+0.33

and space heating is provided by a gas-fired furnace, with negligible electricity usage. For US cooling and ventilation, a centralised all-air HVAC system is used.¹⁹ The centralised HVAC system consists of an outdoor condenser/compressor unit and an indoor air-handling unit. When no cooling is needed, the indoor unit's central fan provides ventilation. The air conditioner system is controlled by a proportional controller, with the input signal from a temperature sensor located in the central exhaust air duct, with the minimum and maximum set points for cooling at 24°C and 25°C , respectively. The maximum air conditioner flow rate is 390 L/s (including outdoor fresh air and recirculating air), based on the target flow rate of $47\text{--}60.5 \text{ L/s/kW}$ of rated cooling capacity.²⁰ The rated cooling capacity of the air conditioner used in the simulation is 7.95 kW, and it uses a variable flow rate depending on the cooling load. As in the Borås case, 60 L/s outdoor fresh air is used for ventilation to ensure the indoor air quality. Thus, the same amount of outdoor air, that is, 60 L/s, is always supplied to the house and mixed with the room air.

3.1.1 | Borås, Sweden

Figure 3A shows the normalised (per unit, 'p.u.') moving average of load and PV-generated power for the studied case in Borås, Sweden. The house is equipped with 14 PV modules (each at 260 Wp), with a total generation of 3583 kWh (AC) and with a total user load demand of 10,744 kWh. Here, it is evident that there is a clear seasonal mismatch between the load usage and PV generation, where the former has its peaks during the heating period (October–March) and the latter during the summer period (May–August). Using the Pearson coefficient correlation from (9) gives a correlation between the PV and load usage of -0.31 , which means a (slight) negative correlation (see Table 1).

3.1.2 | Phoenix, USA

Figure 3B shows the normalised (p.u.) moving average of load usage and PV generation for Phoenix, USA. Here, the PCC from (9) is -0.18 for all loads (see Table 1). This means that the total load usage correlates to the availability of the PV generation slightly better than the case of Borås, Sweden.

In Figure 4, the intraday correlation between PV and load usage is shown for both cases and two arbitrary days with high PV output. Total load demand is shown, divided per category, together with the PV generation and the grid interaction (import and export of power) with and without battery storage 'Grid—battery' and 'Grid', respectively. For Borås (Figure 4A), the lack of load demand around noon generates a poor match with the availability of PV and feeds excess PV to the grid without the presence of a battery (see 'Grid'). When a battery

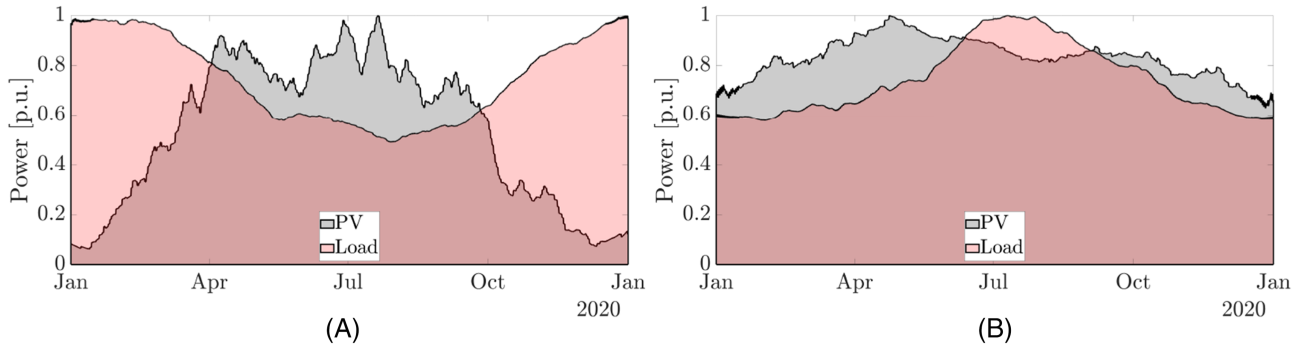


FIGURE 3 Normalised moving mean values of load and PV powers for 1 year in (A) Borås, Sweden, and (B) Phoenix, USA

is added to the same system, the grid interaction is reduced (see 'Grid–battery'), and excess PV energy after noon is stored in the battery and then fed to the loads later in the evening. For Phoenix, the cooling demand is well correlated with the PV generation (see Figure 4B), and the effect of adding a battery is seen where excess generation during midday is stored and used to reduce the grid import during the afternoon/evening. For the Phoenix case, using (9) only on the cooling demand, neglecting household electricity and electricity for DHW production, gives a positive (+0.33) correlation, meaning that the demand is positively correlated to PV generation (see Table 1).

3.2 | System modelling

To evaluate the energy savings from a DC distribution system for the two cases defined in Section 3.1, the building's performance is evaluated for an entire year's operation using the load and PV time-series profiles. The study is made for two system configurations with regard to PV and battery sizes⁵:

1. 3.6/0 kWp/kWh
2. 3.6/7.5 kWp/kWh

where the selected battery size is made from studying the battery 'effectiveness' defined in Pilz et al,²¹ quantifying the increase in self-consumption[†] per kWh added battery size as

$$e_{\text{battery},i} = \frac{SC_n - SC_1}{q_{\text{battery},n}} \quad (10)$$

where SC_n is the self-consumption for battery size $q_{\text{battery},n}$ and SC_1 the self-consumption for the smallest battery modelled. Using this methodology, the highest effectiveness gives the optimal battery for the studied system. Thus, for the load and PV profiles in Borås, this value is achieved at 7.5 kWh. The results from the two cases at the same location give the added energy savings when including battery storage. Comparing Cases 1 and 2 at the two locations quantifies the impact of the geographical location and more specifically the impact from the PV and load correlation.

As results from previous studies have proven the importance of limiting the grid-tied converter throughput to maximise the performance of a DC topology,^{2,4,9} the battery's objective function is set

to maximise the system's self-consumption[#] of generated PV energy. Thus, the modelling is done using the 'Target Zero' dispatch algorithm adopted from Fares and Webber,²² where the battery is only allowed to charge from PV surplus and discharge directly to the load. Thus, no direct interaction is made between the battery and the electrical grid.

The battery's internal losses are modelled using the representation from Ollas² and the measured characteristics of the internal resistance as a function of current throughput. This is to give an accurate representation of the battery's losses under varying operating conditions. In the same manner, the converter's efficiency as a function of its loading has been adopted from the same reference to increase the accuracy of the modelled losses. In Ollas,² it was also concluded that the cable conduction losses are negligible compared to the other sources, and thus, these have been neglected in this study for both system configurations.

For the modelling of the PV output, the System Advisor Model (SAM)[‡] software was used to acquire the PV-generation profiles. For Borås, Sweden, the PV array was modelled with a tilt angle of 41° (from horizontal), and for Phoenix, USA, a tilt angle of 28° was used.²³ Both systems were modelled with an array orientation due south (180° azimuth angle).

Generated PV energy is subject to losses in the inverter. Thus, modelled PV energy, given as AC, is compensated to the DC equivalent using the following relation:

$$e_{\text{PV,DC}}(t) = \frac{e_{\text{PV,AC}}(t)}{\eta_{\text{inv}}(t)} \quad (11)$$

where the inverter efficiency as a function of its loading, $\eta_{\text{inv}}(t)$, is taken from Notton et al,²⁴ as

$$\eta_{\text{inv}}(t) = \frac{p(t)}{m \cdot p(t)^2 + p(t) + p_0} \quad (12)$$

with p_0 and m calculated from the efficiencies at 10% and 100% loading (see Notton et al.²⁴ for numerical values for m and p_0) and with the loading ratio, $p(t)$, calculated as

$$p(t) = \frac{p_{\text{out}}(t)}{P_{\text{rated}}} \quad (13)$$

where $p_{\text{out}}(t)$ is the inverter output and P_{rated} the rated power of the inverter. In this case, a DC/AC ratio of 1.25 is used for the inverter rated power.

⁵It is assumed that the battery power is 80% of its storage capacity, for example, 7.5 kWh = 6 kW.

[†]Self-consumption is defined as the share of PV-generated energy that is used to cover the load demand.

[#]The authors are aware that energy cannot be consumed according to the first law of thermodynamics. But the terminology is used here to match the literature.

[‡]NREL—System Advisor Model—<https://sam.nrel.gov/>.

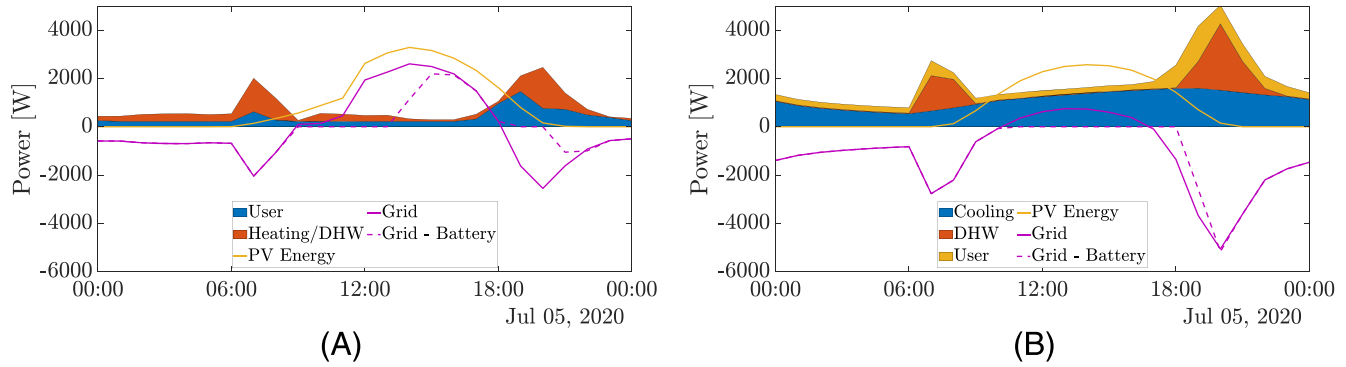


FIGURE 4 Intraday correlation between electrical load demand and PV generation, and resulting grid interaction with ('Grid–battery') and without ('Grid') the inclusion of a battery for (A) Borås, Sweden, and (B) Phoenix, USA. Total load is divided into cooling (only available in Phoenix), domestic hot water (DHW), heating (only for Borås) and household appliances ('User'). For Borås, heating and DHW production are both done by the same sources (ground-source heat pump and an electrical backup heater)

3.3 | Investigated system topologies

The systems are compared for two topologies, AC and DC, where the power distribution is made with 230 VAC and 380 VDC, respectively. In both cases, it is assumed that the smaller loads** have an additional DC/DC conversion from 380 to 24 VDC with the efficiency $\eta_{DC/DC}$ (see Figures 1 and 2). The two topologies compared are

- **230 VAC—reference**

Conventional system commonly used in today's buildings, with a 230 VAC voltage distribution (see Figure 1 for system layout including a PV and battery system).

- **DC—380 VDC**

Voltage distribution at 380 VDC, and this level is selected using the EMerge Alliance 380 VDC standard for data centre power distribution^{25–27} and is the result of an expert assessment of suitable DC distribution levels from Glasgo et al.²⁸ Here, the efficiency of the grid-tied bidirectional converter is modelled for two different cases:

1. with a varying efficiency as a function of the converter's loading, as presented in Ollas²—'DC₁';
2. fixed efficiency of 97.8%²⁹ as commonly done in other related literature^{3,4,7,8,10}—'DC₂'.

where cases DC₁ and DC₂ show the impact of assuming a varying and fixed efficiency respectively for the grid-tied converter.

3.3.1 | System performance evaluation

For a comparison of the system's performance, the overall system efficiency is adopted from Gerber et al.³⁰ For this specific study, the system's efficiency is defined for both the AC and DC topologies as

$$\eta_{\text{system},i} = 1 - \frac{E_{\text{losses},i}}{E_{\text{load}}} \quad (14)$$

where $E_{\text{losses},i}$ are the total annual energy losses for system 'i' and E_{load} the annual energy usage by the loads. †† The system's total energy

demand, $E_{\text{demand},i}$ is thus calculated as

$$E_{\text{demand},i} = E_{\text{load}} + E_{\text{losses},i} \quad (15)$$

The utilisation of the PV energy is calculated from the losses associated with the battery storage, the PV inverter†† and the battery's internal losses (since battery charging is only done through excess PV) and is valid for both the AC and DC topologies. This quantifies the share of useful PV energy that is fed to the system and is expressed as

$$\eta_{\text{PV,system}} = 1 - \frac{E_{\text{inv}} + E_{\text{batt}} + E_{\text{batt,conv.}}}{E_{\text{PV,DC}}} \quad (16)$$

where the PV inverter losses, E_{inv} , are given from (12), E_{batt} is the modelled internal losses from the battery using the representation of a dynamic internal resistance as a function of current from Ollas,² $E_{\text{batt,conv}}$ is the modelled battery converter losses and $E_{\text{PV,DC}}$ is the total DC output from the PV array.

4 | RESULTS

A breakdown of the loss contributions for the two PV and battery systems in Borås, Sweden, is shown in Figure 5A,B. Here, it can be noted that the main loss contributor for the DC case is the grid-tied bidirectional converter and that the inclusion of a battery storage reduces the losses through the same by increasing the self-consumption of the PV energy. Comparing the two DC cases with a varying (DC₁) and fixed (DC₂) grid-tied converter efficiency, the losses in the latter case are underestimated by 14.7% and 19.0% with and without the battery. For this case, the system efficiency gains are 1.2% and 2.7% for DC₁ and 2.3% and 3.6% for DC₂ with and without the inclusion of a battery, respectively, compared to the equivalent AC topology. However, as shown in Ollas,² it is a questionable assumption to use a fixed grid-tied converter efficiency when studying these dynamic scenarios with varying converter loading, and thus, DC₂ is not studied further in this article.

Table 2 gives a numerical comparison of the results for Borås, Sweden, for the AC and DC₁ cases. Here, results show that the inclusion

** Smaller loads are defined as loads with a maximum power of 100 W.

†† Annual energy demand, $E_{\text{load},i}$ is equal for all modelled cases at the same geographical location (see Table 1).

** In the DC topology, there is only a need for a DC/DC conversion from the PV array, and thus, the terminology 'inverter' is only true for the AC topology.

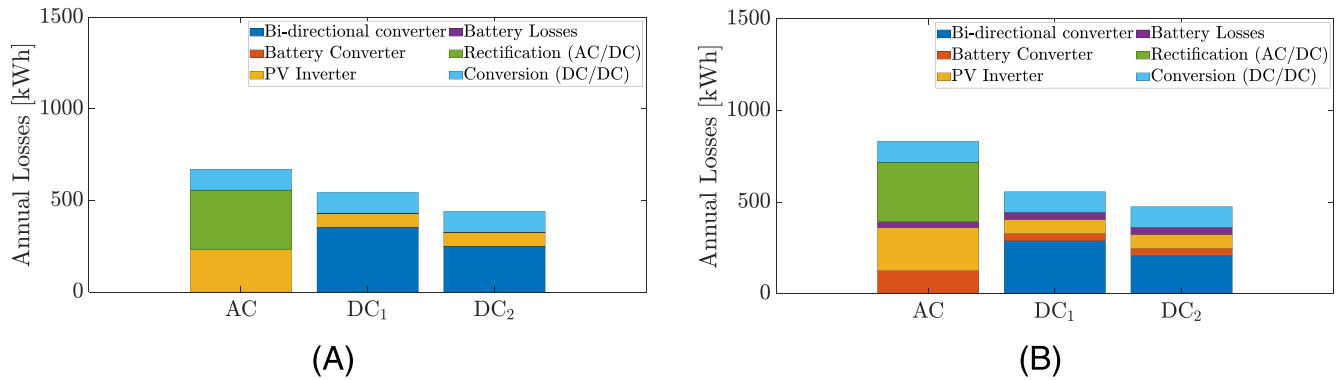


FIGURE 5 Result comparison showing total annual system losses for Borås, Sweden, and two PV and battery systems: 3.6/0 kWp/kWh (A) and the impact when adding a 7.5-kWh battery (B)

	PV = 3.6 kWp and battery = 0 kWh			PV = 3.6 kWp and battery = 7.5 kWh		
	AC	DC ₁	Difference (%)	AC	DC ₁	Difference (%)
Annual losses (kWh)	671	544	−19.0	831	556	−33.1
- Bidirectional converter	0	353		0	288	
- Battery converter	0	0		125	39	
- PV	235	77		235	77	
- Battery losses	0	0		35	38	
- Rectification (AC/DC)	322	0		322	0	
- Conversion (DC/DC)	114	114		114	114	
η_{system}	93.8	94.9	+1.2	92.3	94.8	+2.7
$\eta_{\text{PV, system}}$	94.0	98.0	+4.3	89.9	96.1	+6.9

TABLE 2 Numerical summary of the results for Borås, Sweden, with AC and DC distribution and the two modelled PV and battery systems

Note: 'Difference' refers to the comparison between AC and DC for the same PV and battery system.

of the battery increases the loss savings for the DC case, mainly by reducing the losses from the bidirectional grid-tied converter. Since the PV and battery are directly connected to the DC main link, the losses from the battery converter and PV are significantly reduced in the DC case, compared to the AC case where they are subject to higher conversion losses. As the losses in the battery converter and PV array are lower for the DC cases, the PV utilisation factor, $\eta_{\text{PV, system}}$, defined in (16), increases compared to the AC case. This is more prominent when the battery is included, where the PV utilisation increases from 4.3% to 6.9%.

Similarly, the results for Phoenix, USA, are shown in Table 3 together with the loss separation in Figure 6A,B. As in the Swedish case, the DC systems show better performance in terms of both system efficiency, η_{system} , and PV utilisation, $\eta_{\text{PV, system}}$, than the equivalent AC. The comparison shows that the total losses are reduced further in the US case, −43.6% and −28.5% with and without the inclusion of a battery storage. Again, for the sake of comparison, DC₂ is included in Figure 6 and gives in this case an underestimation of the grid-tied losses by 29%, stressing the importance of using a dynamic efficiency when modelling these types of systems.

To further investigate the impact of the system performance and the potential gains for a DC network, a sensitivity analysis is made by varying the PV array and battery storage sizes (see Figure 7). A comparison of the system efficiency, η_{system} , PV utilisation, $\eta_{\text{PV, system}}$, and total system losses are made for PV array sizes 3.7, 5 and 10 kWp and for battery sizes between 0 and 10 kWh. In Figure 7A, the increase in PV utilisation is shown for the two locations for different PV and battery sizes. Here, the gains from DC operation in Borås, Sweden, are

higher (4.3–7.4%) than the equivalent system configuration in Phoenix, USA, (3.9–6.8%). The gains also increase with battery size, and the highest gains are seen for the smaller PV array (3.7 kWp). The impact of DC operation gain on system efficiency is seen in Figure 7B, where Phoenix shows higher potential system gains than Borås, ranging between 2.3–8.8% and 1.3–5.9%, respectively. For Phoenix, there is an almost linear increase in performance with the increase in battery size and that the incremental increase is less for Borås. In Figure 7C, the resulting reduction in system losses is presented, where the largest savings are seen for the systems modelled in Phoenix (−27% to 46%), while in Borås, the loss savings are between −19% and 39%. It is worth noting that the loss savings for Phoenix are reduced for the largest PV array (10 kWp). This is mainly because the grid-tied losses increase with an increased PV array. At a certain point, the PV array output exceeds the load demand and available storage capacity, forcing the energy through the grid-tied converter to the grid. This is further evaluated in Figure 8 where the losses from grid interaction (import and export through the grid-tied converter) are shown in a duration diagram for Phoenix (Figure 8A) and Borås (Figure 8B), with a battery storage of 10 kWh and a varying PV array size (3.7–10 kWp). Here, the grid import remains equal for the different PV sizes, but the 10 kWp array generates far greater grid-tied converter losses due to the increase in grid export, especially prominent in the US case caused by a higher yearly solar yield.

Comparing the findings from Borås and Phoenix, the gains in PV utilisation for a DC operated system, compared to an equivalent AC, are higher for the former case, ranging between 4.3% and 7.4%, compared to the USA where the gains are between 3.9% and 6.8%.

TABLE 3 Numerical summary of the results for Phoenix, USA, with AC and DC distribution and the two modelled PV and battery systems

	PV = 3.6 kWp and battery = 0 kWh			PV = 3.6 kWp and battery = 7.5 kWh		
	AC	DC ₁	Difference (%)	AC	DC ₁	Difference (%)
Annual losses (kWh)	908	649	−28.5	1222	689	−43.6
- Bidirectional converter	0	384		0	267	
- Battery converter	0	0		243	77	
- PV	436	151		436	151	
- Battery losses	0	0		71	80	
- Rectification (AC/DC)	358	0		358	0	
- Conversion (DC/DC)	114	114		114	114	
η_{system}	92.4	94.6	+2.4	89.8	94.2	+4.9
$\eta_{\text{PV, system}}$	94.2	98.0	+4.0	90.1	95.9	+6.4

Note: 'Difference' refers to the comparison between AC and DC₁ for the same PV and battery system.

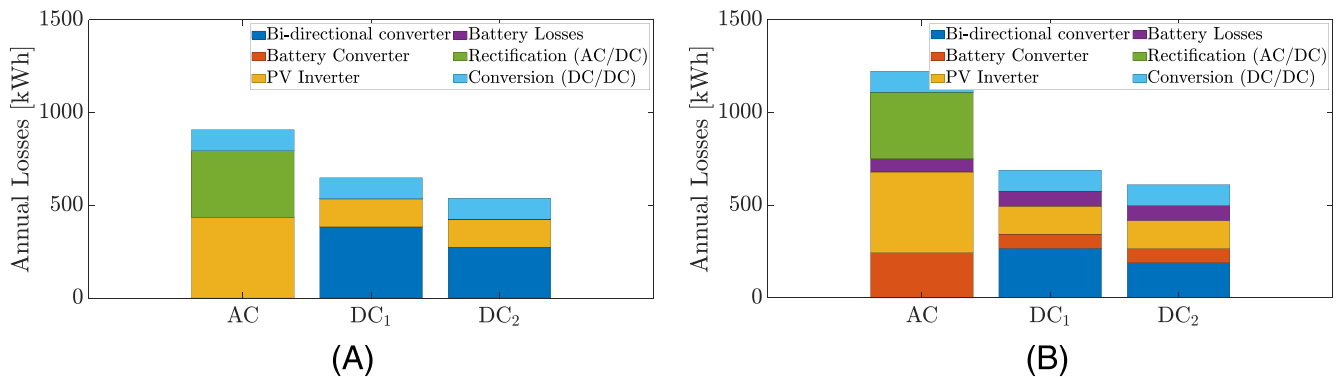


FIGURE 6 Result comparison showing total annual system losses for Phoenix, USA, and two PV and battery systems: 3.6/0 kWp/kWh (A) and the impact when adding a 7.5-kWh battery (B)

However, when looking in absolute terms, the PV is better utilised in the Phoenix case for the larger PV arrays (5 and 10 kWp) as shown in Figure 9. For the smaller array (3.7 kWp), the PV utilisation is higher for Phoenix up until a battery size of 6 kWh and then becomes slightly lower than the equivalent system in Borås.

A summary of literature findings on the DC distribution efficiency improvement potential is given in Figure 10 where either simulations or real demonstrations have been performed to quantify the potential for DC distribution systems compared to equivalent AC systems.^{3-6,9,11,12,31-36} The variance in the results from the literature is due to multiple factors including assumptions of power electronic efficiencies, system topology, the presence and sizing of PV and batteries, modelled or demonstrated results, and so forth. These are compared with the findings from this study for 'Borås, Sweden' (1.3–5.9%) and 'Phoenix, USA' (2.3–8.8%), where the findings from this study are in the lower range of those from the literature.

5 | DISCUSSION AND CONCLUSION

Results show that the potential energy savings for a DC distribution network in a residential building are very much dependent on the grid interaction or, more specifically, the interconnection between supply and demand. The system performance for the residential building in Phoenix, USA, shows an energy efficiency improvement of 8.8–2.3% compared to its equivalent AC system, and in the Swedish case, the gain ranges from 5.9% to 1.3% with and without the inclusion of the battery storage. The utilisation of the PV energy is also increased in

both locations when a DC system is used—in relative terms, the gains are in the range of 7.4–4.3% for Borås and 6.8–3.9% for Phoenix, with and without the battery, respectively. In absolute terms, the generated PV energy in the DC operated systems is better utilised in Phoenix with up to 0.4 percentage points.

Comparing the gains in system efficiency to previous works, the results from this study are in the lower range. An explanation for this could be the assumption made in other studies about using a fixed efficiency for the grid-tied converter, which increases the DC system performance further by reducing the losses from the bidirectional grid-tied converter, as proven in Ollas.² In this work comparing a variable with a fixed efficiency, the losses are underestimated by up to 29% when using the latter. This concludes that when studying these types of dynamic scenarios with power throughput at varying loading levels and considering the load-dependent efficiency, using a constant efficiency is a questionable assumption.

Despite an increase in the PV and load correlation for the US case, the impact from the geographical location has proven to be limited for the PV utilisation. Even though the correlation between supply and demand is increased, the bidirectional converter losses still amount to most of the DC system's losses. From the load usage profiles, it can be noted that the low midday demand generates excess PV energy, especially prominent in the case without the battery, and as this energy passes through the bidirectional converter, it generates losses. Results show that when the PV array is increased to 10 kWp, the losses from the grid export increase substantially compared to the smaller PV sizes, despite the inclusion of battery. This suggests that

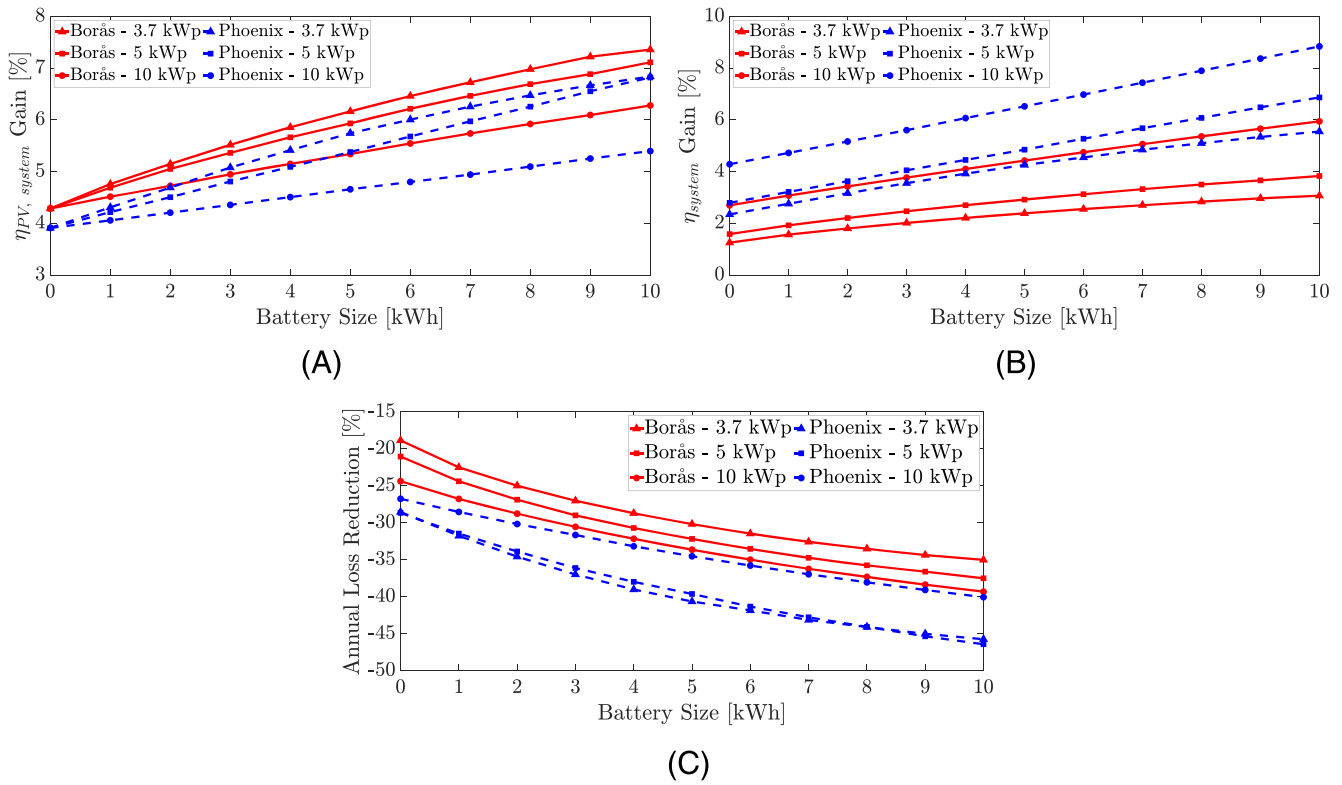


FIGURE 7 Impact on DC performance gains: (A) PV utilisation, (B) system efficiency and (C) total annual system losses, when varying the PV array and battery size for the two locations

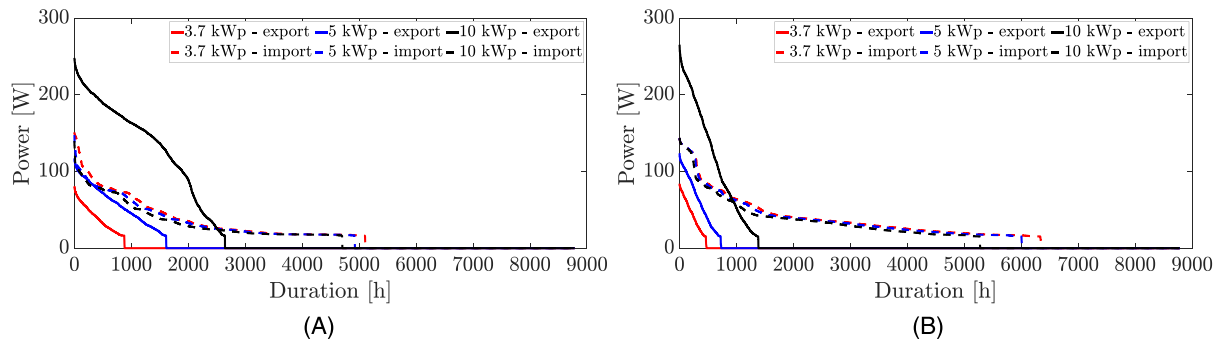


FIGURE 8 Duration diagram of the bidirectional grid-tied converter losses for import and export in (A) Phoenix, USA, and (B) Borås, Sweden, with a 10 kWh battery and varying PV size

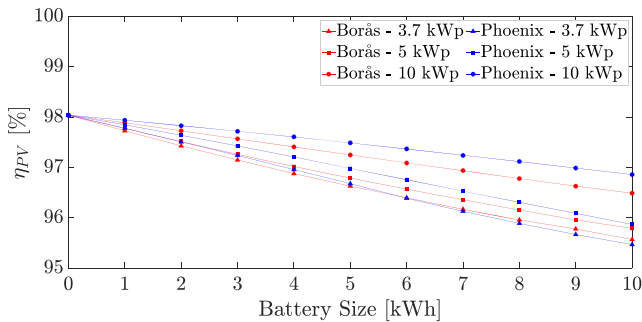


FIGURE 9 PV utilisation factor for DC operation in Borås, Sweden, and Phoenix, USA, for different battery and PV array sizes

the PV and battery sizing are crucial for these types of systems to avoid overgeneration and possible power curtailment.

Studying the PV and load correlations for individual loads suggests that some loads are more naturally correlated with the presence of PV energy, suggesting that DC operation is more suitable for these types. A recommendation for future research, to increase the potential for energy savings from DC distribution, is thus to determine the correlation for each appliance in the building and, for those who correlate poorly, find measures to increase the match, for example, demand response management. Morning and evening load peaks associated with cooking and DHW usage are common in single-family residential buildings, which correlate poorly with south-facing PV arrays. If these loads could be shifted in time—without violating the user needs and thermal comfort too much—to better match the PV, the potential for DC distribution could increase further. Also looking at other types of buildings with peak load demands during midday, for example, office buildings, would be interesting from a DC potential

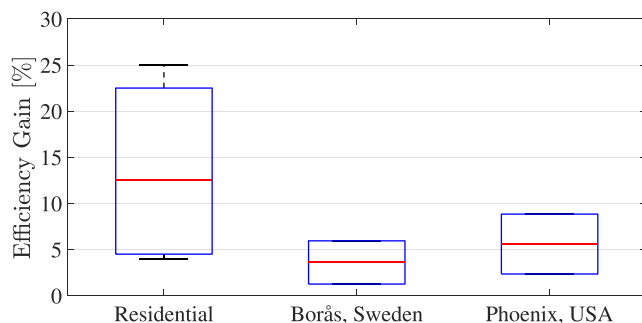


FIGURE 10 DC distribution efficiency gains for residential building found in literature, together with the findings from this study for the two climates, 'Borås, Sweden' and 'Phoenix, USA'. The span is given for the two cases with and without the inclusion of a battery storage

point of view using a south-facing PV array. Another measure would be to change the orientation of the array to better match the load usage profile. In this case study, an east- and/or west-facing array would give a better correlation with the user demand for the studied case and thus reduce the grid interaction and consequently improve the DC performance further.

ACKNOWLEDGEMENT

The authors would like to acknowledge the Swedish Energy Agency ('Energimyndigheten') who has funded this research through Grants 43276-1 and 47273-1.

ORCID

Patrik Ollas  <https://orcid.org/0000-0001-6060-5624>

Torbjörn Thiringer  <https://orcid.org/0000-0001-5777-1242>

Huijuan Chen  <https://orcid.org/0000-0001-7867-5508>

Caroline Markusson  <https://orcid.org/0000-0001-8253-7490>

REFERENCES

- Dastgeer F, Gelani HE, Anees HM, Paracha ZJ, Kalam A. Analyses of efficiency/energy-savings of DC power distribution systems/microgrids: past, present and future. *Int J Electr Power Energy Syst.* 2019;104:89-100.
- Ollas P. Energy savings using a direct current distribution network in a PV and battery equipped residential building. *Licentiate Thesis*: Chalmers University of Technology, Gothenburg, Sweden; 2020.
- Backhaus SN, Swift GW, Chatzivasileiadis S, Tschudi W, Glover S, Starke M, Wang J, Yue M, Hammerstrom D. DC microgrids scoping study. Estimate of technical and economic benefits, Los Alamos National Lab.(LANL), Los Alamos, NM (United States); 2015.
- Denkenberger D, Driscoll D, Lighthiser E, May-Ostendorp P, Trimboli B, Walters P. DC distribution market, benefits, and opportunities in residential and commercial buildings; 2012.
- Glasgo B, Azevedo IL, Hendrickson C. How much electricity can we save by using direct current circuits in homes? Understanding the potential for electricity savings and assessing feasibility of a transition towards DC powered buildings. *Appl Energy.* 2016;180:66-75.
- Hofer J, Svetozarevic B, Schlueter A. Hybrid AC/DC building micro-grid for solar PV and battery storage integration. In: 2017 IEEE Second International Conference on DC Microgrids (ICDCM) IEEE; 2017:188-191.
- Parker L, Maxwell R, Gentry B, Wilder M, Saines R, Camerson J. From silos to systems: issues in clean energy and climate change; 2010.
- Sannino A, Postiglione G, Bollen MathHJ. Feasibility of a DC network for commercial facilities. In: Conference Record of the 2002 IEEE Industry Applications Conference. 37th IAS Annual Meeting (Cat. No. 02ch37344), Vol. 3 IEEE; 2002:1710-1717.
- Seo G-S, Baek J, Choi K, Bae H, Cho B. Modeling and analysis of DC distribution systems. In: 8th International Conference on Power Electronics—ECCE Asia IEEE; 2011:223-227.
- Thomas BA, Azevedo IL, Morgan G. Edison revisited: should we use DC circuits for lighting in commercial buildings? *Energy Policy.* 2012;45:399-411.
- Fregosi D, Ravula S, Brhlik D, Saussele J, Frank S, Bonnema E, Scheib J, Wilson E. A comparative study of DC and AC microgrids in commercial buildings across different climates and operating profiles. In: 2015 IEEE First International Conference on DC Microgrids (ICDCM) IEEE; 2015:159-164.
- Vossos V, Garbesi K, Shen H. Energy savings from direct-DC in US residential buildings. *Energy Build.* 2014;68:223-231.
- Dastgeer F, Gelani HE. A comparative analysis of system efficiency for AC and DC residential power distribution paradigms. *Energy Builds.* 2017;138:648-654.
- Vossos E, Pantano S, Heard R, Brown RE. DC appliances and DC power distribution: a bridge to the future net zero energy homes; 2017.
- Li J, Danzer MA. Optimal charge control strategies for stationary photovoltaic battery systems. *J Power Sources.* 2014;258:365-373.
- Ramadhani UH, Shepero M, Munkhammar J, Widén J, Etherden N. Review of probabilistic load flow approaches for power distribution systems with photovoltaic generation and electric vehicle charging. *Int J Electr Power Energy Syst.* 2020;120:106003.
- Chen H, Markusson C. Demand controlled ventilation in residential buildings. In: Cold Climate HVAC Conference Springer; 2018:111-122.
- Levin P, et al. Brukarindata för energiberäkningar i bostäder. SVEBY, Tech Rep; 2009.
- Stephens B, Siegel JA, Novoselac A. Operational characteristics of residential and light-commercial air-conditioning systems in a hot and humid climate zone. *Build Environ.* 2011;46(10):1972-1983.
- Parker DS, Sherwin JR, Raustad RA, Shirey III DB. Impact of evaporator coil airflow in residential air-conditioning systems. *ASHRAE Trans.* 1997;103:395.
- Pilz M, Ellabban O, Al-Fagih L. On optimal battery sizing for households participating in demand-side management schemes. *Energies.* 2019;12(18):3419.
- Fares RL, Webber ME. The impacts of storing solar energy in the home to reduce reliance on the utility. *Nat Energy.* 2017;2(2):1-10.
- Jacobson MZ, Jadhav V. World estimates of PV optimal tilt angles and ratios of sunlight incident upon tilted and tracked PV panels relative to horizontal panels. *Solar Energy.* 2018;169:55-66.
- Notton G, Lazarov V, Stoyanov L. Optimal sizing of a grid-connected PV system for various PV module technologies and inclinations, inverter efficiency characteristics and locations. *Renew Energy.* 2010;35(2):541-554.
- Alliance E. 380 VDC Architectures for the Modern Data Center. San Ramon, CA, USA: EMerge Alliance; 2013.
- Becker DJ, Sonnenberg BJ. DC microgrids in buildings and data centers. In: 2011 IEEE 33rd International Telecommunications Energy Conference (INTELEC) IEEE; 2011:1-7.
- Geary DE, Mohr DP, Owen D, Salato M, Sonnenberg BJ. 380V DC eco-system development: present status and future challenges. In: Intelec 2013; 35th International Telecommunications Energy Conference, SMART POWER AND EFFICIENCY VDE; 2013:1-6.

28. Glasgo B, Azevedo IL, Hendrickson C. Expert assessments on the future of direct current in buildings. *Environ Res Lett*. 2018;13(7):074004.
29. Thiringer T, Bahmani M, Mannikoff A, Söderbom J, Kharezy M, Hagmar H, Lindskog A. Besparingspotential för likströmsdistribution-en förstudie. Chalmers University of Technology; 2017.
30. Gerber DL, Vossos V, Feng W, Marnay C, Nordman B, Brown R. A simulation-based efficiency comparison of AC and DC power distribution networks in commercial buildings. *Appl Energy*. 2018;210:1167-1187.
31. AlLee G, Tschudi W. Edison redux: 380 Vdc brings reliability and efficiency to sustainable data centers. *IEEE Power Energy Mag*. 2012;10(6):50-59.
32. Gerber DL, Vossos V, Feng W, Marnay C, Nordman B, Brown R. A simulation-based efficiency comparison of AC and DC power distribution networks in commercial buildings. *Appl Energy*. 2017;210:1167-1187.
33. Noritake M, Yuasa K, Takeda T, Hoshi H, Hirose K. Demonstrative research on DC microgrids for office buildings. In: 2014 IEEE 36th International Telecommunications Energy Conference (INTELEC) IEEE; 2014:1-5.
34. Patterson BT. DC, come home: DC microgrids and the birth of the "enernet". *IEEE Power Energy Mag*. 2012;10(6):60-69.
35. Savage P, Nordhaus RR, Jamieson SP. *DC Microgrids: Benefits and Barriers, from Silos to Systems: Issues in Clean Energy and Climate Change*. New Haven, CT: Yale Publications; 2010.
36. Weiss R, Ott L, Boeke U. Energy efficient low-voltage DC-grids for commercial buildings. In: 2015 IEEE First International Conference on DC Microgrids (ICDCM) IEEE; 2015:154-158.

How to cite this article: Ollas P, Thiringer T, Chen H, Markusson C. Increased photovoltaic utilisation from direct current distribution: Quantification of geographical location impact. *Prog Photovolt Res Appl*. 2021;1-11. <https://doi.org/10.1002/pip.3407>